Mixed α-Fe_2O_3/Bi_2WO_6 oxides for Photoassisted Hetero-Fenton Degradation of Methyl Orange and Phenol

C. Jaramillo-Páez[1*], J.A. Navío[1], M.C. Hidalgo[1],
Asmae Bouziani[2], Mohammed EL AZZOUZI[2]

[1]Instituto de Ciencia de Materiales de Sevilla, Centro Mixto Universidad de Sevilla-CSIC, Américo Vespucio 49, 41092 Sevilla, Spain

[2]Department of Chemistry, Faculty of Sciences Rabat, University Mohammed V 4 Avenue IBN BATTOUTA B.P.1014 RPRabat, Morocco.

Abstract

Mixed oxides, α-Fe_2O_3/Bi_2WO_6, were prepared using a mechanical mixing procedure by adding to the Bi_2WO_6previously obtained by hydrothermal method the corresponding amount of a prepared α-Fe_2O_3, the latter obtainedby thermal decomposition of $Fe(NO_3).9H_2O$. The physicochemical surface, structural, morphological characteristics and optical properties of the samples, single and mixed, were determined by BET, XRD, FE-SEM, XPS and UV-Visible diffuse reflectance spectroscopy. UV–vis diffuse reflectance spectra showed that incorporating a 5%wt. of α-$Fe_2O_3$to the corresponding amount of Bi_2WO_6 sample broadened the visible light absorption of Bi_2WO_6as expected. The photocatalytic activity, of single and mixed catalysts, to degrade a selected dye such as Methyl Orange (MO) as well as the transparent substrate Phenol (Ph)were studied, in aqueous medium (pH ≈ 5.5)under UV and sun-like illumination conditions in the absence and presence of H_2O_2. In the present study the use ofaα-Fe_2O_3-Bi_2WO_6/H_2O_2 systemdemonstrate much higher photocatalytic efficiency to degrade both MO and Phthan pristineBi_2WO_6or α-Fe_2O_3, single or mixed. Using the system α-Fe_2O_3-Bi_2WO_6/H_2O_2, around 85% ofMO was degraded in 60 min under sun-like illumination whereas 100% was degraded in 60 min under UV-illumination. However, just around 30% of Ph was degraded in 120 min in the α-Fe_2O_3-Bi_2WO_6/H_2O_2 system under sun-like illumination whereas around a 95% was degraded in 90 min under UV-illumination. Under UV-illumination, the generation of hydroxyl radicals is favorable; whereas under sun-like illumination, only the small fraction of the UV can produces the •OH.Under illumination, the H_2O_2could react with photoinduced electrons from the photocatalysts leading to the production of hydroxyl radicals (•OH).

Keywords:Bismuth Tungstate; Iron oxide; Photocatalysis; Photo-Fenton; Phenol; Dyes; Hydroxyl radicals.

* Corresponding author. Tel.: +34955420998
E-mail address: navio@us.es(J.A. Navío).

1. Introduction

The increase of industrial activities has become a serious problem that leads to the augmentation ofpollution inair, water and soil. To facethis problem, the scientific community works to find new methods to undo thecontamination.During the past few decades, a variety of practical strategies have been implemented to develop viable wastewater treatment technologies[1–6].

Those technologies are very appealing alternatives for the degradation of organic pollutants because they permit a partial or complete mineralization of pollutants. It is based on the production of the very reactive and nonselective entities (particularly the hydroxylradicals•OH) having a higher oxidizing capacity than traditional oxidants (O_2, Cl_2, ClO_2, H_2O_2, O_3…)[7–9].

Photocatalytic degradation of organic pollutants to purity wastewater from industries and household has received extensive attention in recent years. In particular, heterogeneous photocatalysis shows promising potential in depth-oxidation of pollutants to non-toxic inorganic molecules at ambient temperature[10].

Dyes are molecules commonly found in real effluents from textile and other industrial wastewaters[11,12]. Dyes are major organic pollutants, which can cause severe environmental disruption and health damages[13]. Similarly, phenol is one of the most abundant pollutants in industrial wastewaters and its toxicity, carcinogenicity and persistence, makesthiscompound dangerous for life at rather low concentrations. In this sense, heterogeneous photocatalysis, among a group of available technologies known as advanced oxidation

processes (AOPs), is an important alternative to remove a wide range of organic compounds, including phenolsand dyes, in polluted streams. Other technologies as Fenton and Photo-Fenton have been successfully used in depollution of water[14–18].

To meet the requirement of future environmental applications, in the field of AOPs, it is still essentialto not only further improve the photocatalytic activity by synthesizing new photocatalysts but also to explore new combined processes.
The development of new photocatalysts is attracting vast interest. Among them the Bismuth tungstate (Bi_2WO_6) is a typical n-type direct band gap semiconductor with a band gap of 2.8 eV and has prospective applications for the degradation of organic pollutants under visible light illumination due to their low valence band and high chemical stability[19]. In the same context, iron oxide (α-Fe_2O_3, hematite) with a narrow band gap at 2.2 eV, absorbing the light up to 600 nm and collecting about 40% of the solar spectrum energy, is also another of the promising materials for photocatalytic applications[20].

H_2O_2 is a distinctive oxidative agent and has been frequently used in practical water treatment, because it's a very common source of very active hydroxyl radicals (•OH) by its decomposition after being illuminated with ultraviolet (UV) light.The use of H_2O_2 in photochemical processes (UV/H_2O_2) and UV (H_2O_2/ Fe^{3+} (Photo-Fenton)) has been investigated[1,21–24], however, long periods of UV-illumination are required,thuspoor degree of mineralization isobtained, makingall these processes not perspectives as potential methods for wastewater purification.

From another perspective, as an electron capture agent, H_2O_2 can also react with photogenerated electrons, from a photocatalytic process, to producehydroxyl radicals (•OH) as established in eq. (1-2) in which (SC) is a general semiconductor photocatalyst[25].

$(SC) + h\nu \rightarrow (SC)(e^-_{CB} + h^+_{VB})$ (light absorption) (eq. 1)

$(H_2O_2) + e^-_{CB} \rightarrow \bullet OH + OH^-$ (eq.2)

$(H_2O) + h^+_{VB} \rightarrow \bullet OH + H^+$ (eq.3)

The formation, the adsorption and the degradation of H_2O_2 on different samples (TiO_2 and ZnO) have been investigated to better understand its participation in the photocatalytic reactions [26]. In a typical UV/H_2O_2/TiO_2 system, the active radical formation can arises not only from the direct UV-photolysiswhich takes place throughahomolytic process (H_2O_2 + hv → 2 •OH) but also from the photocatalytic ones (equation 1 to 3).

Thus, if the photocatalyst only absorbs in the UV region, then the hydroxyl radicals photogeneration, during the combined photochemical process UV/(SC)/H_2O_2, can take place not only by the homogeneous photolytic decomposition of H_2O_2, but also according to the processes indicated in equations 1 and 2. But if the photocatalyst absorbs in the visible region, the generation of hydroxyl radicals (OH^-)would be expected to occur, under visible illumination,by the photogenerated electron capture of H_2O_2, since the photolytic decomposition of H_2O_2 requires shorter wavelengths[1].

The generation of H_2O_2 and hydroxyl radicals on Bi_2WO_6 for phenol degradation under visible light has been reported [27]. From this work, Authors concluded

that the observed organic degradation over the irradiated Bi_2WO_6 in aerated aqueous solution is due to the production of •OH and H_2O_2.

Both photocatalysts, Bi_2WO_6 and α-Fe_2O_3, display potential catalytic activity to many chemicals organic degradation under conditions of sun-like illumination. However, due tothe high recombination rate of photogenerated charge carriers, the ability isthereof limited. Various strategies, such as heterostructured constructing are being developed[28–30].

The aim of this work is not focused on developing a α-Fe_2O_3/Bi_2WO_6heterostructure, but to use a physical mixture of both materials and explore their photochemical activity in the presence or absence of H_2O_2 in the degradation of two selected substrates.

Therefore, when H_2O_2 is co-present with single or physically mixed $Bi_2WO_6$and α-Fe_2O_3, different activities could be displayed because, parallel to the mechanism of homogeneous degradation by hydroxyl radicals photogenerated by H_2O_2,the effect generated by the intrinsic photocatalytic activity of single or mixed systemsisalso expected to occur.

Methyl orange (MO) and phenol (Ph) are used to imitate non biodegradable, toxic organic compounds. The photocatalytic activity, under UV or sun-like Illumination, of α-Fe_2O_3, Bi_2WO_6 and mixed α-Fe_2O_3/Bi_2WO_6 samples,to Methyl Orange and Phenol degradation, in the absence and presence of H_2O_2 is reported.

2. Experimental details

2.1 Preparation of α-Fe_2O_3, Bi_2WO_6 and mixed α-Fe_2O_3/Bi_2WO_6 samples

All the reagents used in this procedure were analytical grade without further purification. The detailed synthesis procedure for single α-Fe_2O_3, Bi_2WO_6 and mixedα-Fe_2O_3/Bi_2WO_6 sample was as follow: The iron oxide was prepared by drying iron(III) nitrate nonahydrate $Fe(NO_3).9H_2O$ at 120°C for 2h then submitting the samples to a further calcinations treatment at 300°C for 2h.

The Bi_2WO_6 was prepared according to the method previously described [31]by dissolving 4.85 g of $Bi(NO_3)_3.5H_2O$ in 10 mL of glacial acetic acid, and 1.7 g of $Na_2WO_4.2H_2O$ in 90 mL of distilled water, then those two solutions were mixed forming a white suspension (pH≈2), which was kept under stirring for 1h. The white suspension was transferred into a Teflon recipient insideastainless steel autoclave.The hydrothermal treatment was done at 140°C for 20h, and then the precipitate was filtered, washed and dried overnight at 120°C. Finally the sample was submitted to a calcination treatment at 300°C for 4h.

The α-Fe_2O_3/Bi_2WO_6 mixed samples were obtained with a mechanical mixing in agate mortar, by adding the prepared α-Fe_2O_3 to the corresponding amount of Bi_2WO_6 for a 5wt. % of iron oxide in the mixture. This sample will hereafter be named as BW-Fe(5)-2 indicating a 5% of iron oxide and that Bi_2WO_6 was prepared at pH=2.

2.2. Characterization of the photocatalysts

BET surface areas (S_{BET}) of all samples were evaluated by N_2 adsorption measurement with a Micromeritics ASAP 2010 instrument. Degasification of the samples was performed at 150 ºC for 30 min in He flow.

Crystalline phase composition of the samples was estimated by X-ray diffraction (XRD). XRD patterns were obtained on a Siemens D-501 diffractometer with Ni filter and graphite monochromator using Cu Kα radiation.

The morphology for all the samples was analyzed by field Scanning electron microscopy (FE-SEM) using a Hitachi S 4800 microscope.

Light absorption properties of the samples were studied by UV–Vis spectroscopy. The Diffuse Reflectance UV–Vis Spectra (UV–Vis DRS) were recorded on a Varian spectrometer model Cary 100 equipped with an integrating sphere and using $BaSO_4$ as reference. Band-gaps values were calculated from the corresponding Kubelka–Munk functions, $F(R\infty)$, which are proportional to the absorption of radiation, by plotting $(F(R\infty)\times h\nu)^{1/2}$ against hv.

X-ray photoelectron spectroscopy (XPS) studies were carried out on a Leybold-Heraeus LHS-10 spectrometer, working with constant pass energy of 50 eV. The spectrometer main chamber, working at a pressure $<2\times10^{-9}$Torr, is equipped with an EA-200 MCD hemispherical electron analyzer with a dual X-ray source working with Al Kα (hv=1486.6 eV) at 120 W and 30 mA. C1s signal (284.6 eV) was used as internal energy reference in all the experiments. Samples were outgassed in the pre-chamber of the instrument at 150 ºC up to a pressure $<2\times10^{-8}$Torr to remove chemisorbed water.All photoelectron spectra were analyzed using Casa-XPS software.

2.3. Photodegradation tests

The photocatalytic activity of the catalysts prepared was tested in the photo-discoloration of a selected dye, Methyl Orange (MO), as well as on the photodegradation of Phenol (Ph) as a selected transparent, toxic

substrate.Methyl Orange and Phenol (ReagentPlus >99%) were supplied by Sigma-Aldrich.Photocatalytic tests were carried out using a discontinuous batch system, this includes a 250 mL Pyrex reactor enveloped by an aluminum foil, filled with an aqueous suspension (100 mL) containing either the single substrates (concentrations: 20 ppm of MO or 50 ppm of phenol) or a mixture of both (10 ppm of MO/25 ppm phenol) and the photocatalyst (1g/L). On the experiments in which H_2O_2 is co-present, either with substrates or with substrates and catalysts, before illumination, a certain amount (~ 3 mM) of H_2O_2 (wt. 30%) was added in the medium. The mixed solution was magnetically stirred in the dark for 20 min. Systems were illuminated through a UV-transparent Plexiglas® top window (threshold absorption at 250 nm) by an Osram Ultra-Vitalux lamp (300 W) with sun-like radiation spectrum and a main line in the UVA range at 365 nm. The intensity of the incident UV-Visible light on the solution was measured with a Delta OHM photo-radiometer HD2102.1, being ca. 110 W/m^2 whereas the intensity of the incident UV light on the solution was of ca. 90 W/m^2. In order to favor the adsorption–desorption equilibrium between the catalysts and substrates, prior to irradiation the suspension was magnetically stirred for 20 min in thedark. Magnetic stirring and a constant oxygen flow of 20 L/h, as an oxidant, were used to produce a homogeneous suspension of the photocatalyst in the solution. A tank bubbler was used as a source of natural oxygen. All photocatalytic tests started at pH ca. 5.5 and the total reaction time was 120 min.

During the Methyl Orange photoreaction, samples were collected at different times and in order to evaluate the dye discoloration rate, the concentration of Methyl Orange during the photodegradation reaction was analyzed by UV–

Visible spectroscopy, considering the main peak of this dye in the visible range, located at 465 nm. For this analysis a UV–vis spectrometry with a Cary 100 (Varian) spectrometerwas used.

Phenol concentrations were followed by HPLC technique (Agilent, 1200 Series) using anElipse XDB-C18 column (4.6 x 150 mm i.d., 5 μm; Agilent) at 40ºC. Mobile phase was water/methanol (65:35) at a flow rate of 0.8 ml/min. Samples of about 2 mL were removed periodically during the experiment and filtered (Millipore Millex 25 0.45 mm membrane filter) previous to HPLC measurements. Photolysis tests of substrates under illumination and in absence of catalyst were carried out. Under the experimental conditions used in this work, substrate photolysis was negligible. Reproducibility of the measurements was ensured by double testing of selected samples.

Total organic carbon was followed also by means of a TOC analyzer (Shimadzu 5000). Mineralization degrees (%) were evaluated by the TOC values upon 2 h of illumination,for all the photo-assisted processes studied.

3. Results and discussion

3.1. Characterization

Figure 1 shows X-ray diffraction patterns (XRD) of the prepared materials.The XRD of the as-prepared iron oxide sample showed the diffraction peaks corresponding to the standard α-Fe_2O_3 (JCPDS no. 33-0664). The main peaks at 24.1, 33.1, 35.6, 49.5 and 54.1º was observed, which correspond to (012), (104), (110), (024) and (116) diffraction planes of hematite respectively. For the Bi_2WO_6 sample all the diffraction peaks are in good consistent with the standard data of the pure russelite orthorhombic Bi_2WO_6 phase (JCPDS no. 39-0256).

However, the XRD spectra of the prepared mixed oxides BW-Fe(5)-2 sample, only shows diffraction peaks indexed to the pure orthorhombic Bi_2WO_6 phase but not diffraction characteristics of α-$Fe_2O_3$was detected in the XRD of the BW-Fe(5)-2 sample. The plausible reason is that the little content ofα-$Fe_2O_3$is beyond the detection limit of XRD measurements.However the presence of iron oxide was confirmed by XPS.

No characteristic peaks of any impurities are detected and the sharp diffraction peaks imply that good crystallinity occurs.

The UV-vis diffuse reflection spectra (DRS) for the prepared samples were depicted in Figure 2. It can be seen that Bi_2WO_6 presents a photo-absorption in the range from the UV-light to visible-light region shorter than 460 nm, corresponding to the band-gap of 2.8 eV. Pure crystallized α-Fe_2O_3 exhibits a broad absorption in the whole UV-vis region, in which the UV-absorption comes from the direct transition from O^{2-} (2p) to Fe^{3+}(3d) and the visible light absorption is resulted from the indirect transition between Fe^{3+} (3d) electrons as reported in ref. [32]. α-Fe_2O_3 is a n-type semiconductor with a narrow band gap of 2.2 eV, whichcan not only promote the separation and migration of photon-generated carriers, but might also contribute to for a conduction band at a higher position[28].

Compared to pristine Bi_2WO_6, the optical absorption of BW-Fe(5)-2 displays an evident red-shift in the light-visible region, which can be ascribed to the presence of α-Fe_2O_3 in the mixture sample, in spite of iron oxide not being detectedby XRD. In principle, thissuggests that the mixed oxide sample canbe favorablefor the use of sunlight as energy source of pollutants abatement.

The S_{BET} of pure Bi_2WO_6 was about 25.0 m²/g and that of α-Fe_2O_3 was about 18.5 m²/g, whereas for the BW-Fe(5)-2 sample was 16.7m²/g.

FE-SEM pictures of the prepared samples are shown in Fig.3. Bi_2WO_6 showed 3D flower-like spherical superstructures (Fig.3A) with a diameter rangingbetween5-8 μm constructed by sheets aligned perpendicularly to the spherical surface (Fig. 3B) as it was found in other previous studies[33,34].

Figure 3C shows the FE-SEM images of the as-preparedα-Fe_2O_3, in which irregular particles are observed, presenting free and agglomerations of small particles (ca. 0.1 μm) together with irregular laminar particles of different sizes (ca 0.6 μm).

Concerning the morphology of α-Fe_2O_3/Bi_2WO_6 mixed oxides(Fig. 3D) it was relatively comparable to Bi_2WO_6 with the existence of spherical particles of Bi_2WO_6 (ranging 3-4μm) distributed over an agglomerationof small particles (ca. 1μm)matching α-$Fe_2O_3$and bigger sheet of Bi_2WO_6 particles, indicating that on the mix the bigger spherical Bi_2WO_6 particles have beendestructured giving free sheetparticles.

3.2 Photocatalytic activity

3.2.1 Blank experiments: (UV/Sun-like)+H_2O_2

As previously it said, preliminary experiments were carried out in order to verify that substrates (MO and Ph) were removed by the heterogeneous photoassisted processes under UV and sun-like illumination, investigating the effect of H_2O_2 on both substrates under those two lighting conditions.

It was found that in the absence ofthephotocatalyst no decreases in MO or in Ph concentrations wereobserved, under illumination. Therefore photolysisprocesses didn´t occur. Similarly, no significant variations in the initial concentrations of both substrates were found, in dark and in the presence of H_2O_2.

However, as shown by results in Figure 4A, the simultaneous presence of H_2O_2 and light has a marked influence on the discoloration process of MO.This effect is more pronouncedunder conditions of UV-illumination for which100% discoloration is achievedin 60 min.

Similar experiments were performed for Phenol in the presence of H_2O_2 under UV or sun-like illumination. Figure 4B presents the results of both experiences. As shown, photochemical disappearance of Phenol, in the presence of hydrogen peroxide, also generates significant conversionvalues being themost effective processthe oneunder UV illumination in comparison to the one under sun-like illumination. However, the 100% for Phenol conversion in the presence of H_2O_2 is achieved only after a long time (120 min) of UV lighting.

At this point, it is interesting to note that although duringthe UV-H_2O_2photochemical processes, high conversion rates of MO and Ph are obtained; it is nevertheless surprising that after 120 min of illumination in the presence of H_2O_2, relatively high values of TOC are obtained for both substrates, from which the mineralization percentages were calculated and they are contained in Table 1. So, in the presence of H_2O_2 under UV-illumination the percentage of MO mineralization was 54%, being ca. 39% for the same substrate under sun-like illumination.For phenol, the mineralization degrees

were lower: 49% under UV illumination and ca. 26% under sun-like illumination.These results clearly indicate that conversions values obtained, do not imply a process of complete mineralization of the substrates.As mentioned above, long periods of UV-illumination are required toobtain a certain degree of mineralization.

However, all these experiments serve as reference targets to rationalize the results obtained in the presence of photocatalysts studied.

3.2.2 Bi_2WO_6 and Bi_2WO_6-H_2O_2

In Fig. 5, we show the conversion plots of single substrates, MO or Ph, using the Bi_2WO_6 synthesized catalyst, under UV or sun-like illumination, in the absence (Fig. 5A and 5B) or in the presence of H_2O_2 (Fig. 5C and 5D). It is observed that both single substrates present almost negligible conversionvalues (less than 10%) over the whole (120 min) illumination period, bothin UV andsun-like illumination conditions, though with this catalyst under UV illumination there is a slight improvement inPhenol (Fig.5B) compared with that obtained with MO (Fig.5A).

While, very low activities of the photocatalyst used on the two substrates were observed, also very high values of TOC are obtained, indicating poor photocatalytic degradation.In fact, for MO, a mineralization degree of 14.6 % was obtained under UV-irradiation, being of 5.5 % under sun-like irradiation.

As mentioned above,band-gap illumination of semiconductor (SC) water suspensions produces electron-hole (e^--h^+) pairs (equation 1) which can react

with species present in solution giving rise to redox reactions. If oxygen is present, its reduction by conduction band electrons is possible and an oxidable substrate (S) can be attacked directly by holes as indicated by equations (4 and 5):

$((SC)(e^-_{CB})+O_2(ads.)\rightarrow (SC) + O_2^-(ads.)$ (electron trapping by O_2 ads.) (eq.4)

$(S)_{ads} + h^+ \rightarrow (S)_{ads}^{\cdot +} \rightarrow$ Byproduct + (Final products) (eq.5)

However, the low photocatalytic efficiency shown by Bi_2WO_6, should be understood in terms of a high recombination rate of charge carriers, photogenerated in the process of radiation absorption (equation 6).

$(SC)(e^-_{CB}+ h^+_{VB}) \rightarrow (SC)$ (charge recombination) (eq. 6)

The co-presence of H_2O_2 with Bi_2WO_6 catalyst, notably changes photo-conversion processes (Figures 5C and 5D). Better conversions are observed in this experimental condition, both for MO and for Phenol,which should be attributed to the co-presence of H_2O_2. It is remarkableto note that higher conversions are obtained under UV-illumination. Thus whereas for MO, using Bi_2WO_6-H_2O_2, a practically 100% of disappearance of MO was achieved in 60 min of UV-illumination, whileonly a 70% was obtained for Phenol under the same conditions. For both singles substrates, around 45% of conversions were obtained after 120 min under sun-like illumination.

However, if we consider the preliminary results shown in Figure 4A, we can infer that the improvement obtained is due solely to the presence of H_2O_2 under illumination. The catalyst, in this case bare Bi_2WO_6, does not seem to exert any positive effect on the process of photo-bleaching MO.

By comparing the results obtained for Phenol disappearance with the catalyst Bi_2WO_6, in the co-presence of H_2O_2 (Fig.5B), with those obtained only with H_2O_2 in the absence of catalyst (Fig. 4B) it can be inferred that also, in this case, no marked influence is observed by the simultaneous presence of catalyst and H_2O_2, obtaining practically the same values for Phenol disappearance after a period of 120 minutes of illumination both under UV and sun-like.

These results indicate that if one takes into account the possibility that the mechanism indicated byequations 1 and 2 occur, they don'tseem favourable due to high recombination of photoinduced charge carriers, whereby the electron capture process by H_2O_2, indicated in equation 2, does not seem favourable.

Bytaking into account the TOC values measured for each process, after 120 min of illumination, it can be inferred that although the degree of conversion obtained in the photochemical process using Bi_2WO_6-H_2O_2 are analogous to those obtained in photochemical processes with H_2O_2 alone,better values of mineralization degree areobtainedfor both substrates(Table 1). Thus, under these conditions (Bi_2WO_6-H_2O_2), for MO, a mineralization degree of 68.1% was obtained, with bothUV andsun-like irradiation. For Phenol, a mineralization degree of 68.3 % was obtained under UV whereas a value of 55.2 % was achieved under sun-like illumination.

This suggests that there is a better synergy effect in the Bi_2WO_6-H_2O_2 system, under sun-like illumination, for degradation of the dye, than for the phenol.The differences observed may be associated with physical-chemical properties of the catalyst and/or with the hydroxyls groups´ population at the surface of

catalysts, which obviously condition the capacity of surface adsorption for substrates of different chemical natures. In fact, according to the results reported in the literature [26], the adsorption capacity of H_2O_2 seems to be linked to the number of OH groups present on the surface of solids.

Regardless of this, it is evident that the Bi_2WO_6-H_2O_2 system increases the degrees of mineralization of both substrates, with respect to those obtained when only the catalyst or H_2O_2 are used.

A proposed mechanism to explain the combined process of Bi_2WO_6 and H_2O_2, would be the generation of hydroxyl radicals, either by capturing electrons by H_2O_2 and the simultaneous oxidation of H_2O by holes, as stated in the equations 1 to 3 in which the semiconductor (SC) would be Bi_2WO_3, as well as by the direct photolytic processes (H_2O_2 + hv → 2 OH.).

3.2.3 α-Fe_2O_3 and α-Fe_2O_3-H_2O_2

Figure 6A shows the processes in the dark and under illumination, which occur for MO substrate in the presence of α-Fe_2O_3. As can be seen in the dark, a large adsorption of MO occurs at the surface of α-Fe_2O_3. A tentative explanation of the adsorption process in the dark would be the establishment of a weak Lewis acid-base interaction between the electron density of the chromophore group (-N=N-) and *d*-orbitals of Fe^{3+}.After equilibration, the backlight, both in the UV and sun-like, generates a photo-desorption process of the MO.These photo-desorption processes are accompanied by photocatalytic degradation processes of MO, since after 120 min under lighting conditions TOC values obtained indicatethat there has been a percentage of 27.4% of

mineralization(Table 1).However, as the TOC measurement is performed on the liquid phase, it is also possible that MO is not completely desorbed and this apparent decrease on TOC could not be related to a mineralization.

This fact is important since iron is the second most abundant metal on Earth, and the mineral hematite is most often formed in natural water. Thus, a natural photocatalytic degradation process with particles of α-Fe_2O_3 suspended in water or sediments could have a beneficial impact to the water ecosystem contaminated by MO.

In the degradation test of MO with α-Fe_2O_3, an initial adsorption and later desorption under illumination is observed (Figure 6A).This behavior observed for the MO in the presence of α-Fe_2O_3, is not observed when Phenol is used. Figure 6B shows the plot of the conversion percentages of Phenol, using the prepared catalysts α-Fe_2O_3.As with the use of Bi_2WO_6, the use of α-Fe_2O_3 leads to conversion percentages which are negligible for both substrates, both under UV and sun-like illumination. These results indicate that the as prepared iron oxide sample presents, not only a low adsorption capability for Phenol but also a low photoactivity, although optical absorption results, by DRS (Fig.2), indicate a wide optical absorption both in the ultraviolet and in the visible, being in accordance with the narrow band gap at 2.2 eV. The poor photoactivity, tested for the prepared α-Fe_2O_3, similarly to that observed for Bi_2WO_6, could be associated with the high recombination of charge carriers in the prepared samples.It is interesting to note that although nosignificant degrees of conversion for phenol were observed, however TOC values indicate that there has been a certain degree of mineralization (25-35%) for phenol(Table 1).

It is interesting to note that the simultaneous presence ofthe catalyst (α-Fe_2O_3) and H_2O_2, leads toa significant increase in conversion percentages for both substrates, both in the UV and the sun-like (Figures 6C and 6D) and that they are different from those obtained for the twosubstrates both withonly the catalyst (Figures 6A and 6B) and with H_2O_2 alone (Figures 4A and 4B).These results are not surprising if they are explained in the context of a photoassisted hetero-Fenton process implemented by the α-Fe_2O_3/H_2O_2 system.Thus,regardless of whether the H_2O_2-photolytic process generating •OH radicals (equation 7), the α-Fe_2O_3/H_2O_2 systemwould also be acting by generating more hydroxyl radicals via a simultaneous heterogeneous photo-Fenton mechanism involving Fe^{3+}/Fe^{2+} pairs, as the following:

$H_2O_2 + hv \rightarrow 2•OH$(eq. 7)

$>Fe^{3+} + e^- \rightarrow >Fe^{2+}\ [O_2] \rightarrow >Fe^{3+}$(eq. 8)

$>Fe^{2+} + H_2O_2 + H^+ \rightarrow >Fe^{3+} + •OH + H_2O$ (eq. 9)

$>Fe^{2+} + •OH \longrightarrow >Fe^{3+} + OH^-$(eq. 10)

$>OH^- + h^+ \rightarrow •OH$(eq. 11)

In the presence of oxygen, re-oxidation of $>Fe^{2+}$ occurs at a high rate before detaching from the surface (photocorrosion).For this reason, the photocorrosion of iron oxide in photocatalytic reaction (under oxygen) is generally very low with this process being hindered[35–37]**.**

3.2.4 α-Fe_2O_3/Bi_2WO_6 andα-Fe_2O_3/Bi_2WO_6-H_2O_2

In Fig. 7, we show the MO and Phenol conversion plots using the mixed α-Fe_2O_3/Bi_2WO_6photocatalysts both in the absence (Figures 7A and 7B) or in the presence of hydrogen peroxide (Figures 7C and 7D), under UV and sun-like irradiation. It is possible to observe that using the mixedα-Fe_2O_3/Bi_2WO_6 photocatalysts,MOremains almost unaffected in solutions under illumination. With BW-Fe(5)-2 under these conditions, there is a slight improvement of Phenol conversion, after 120 min of illumination (Fig.7B), compared with that obtained for MO (Figure 7A). However, the small conversion values observed are higher under conditions of UV-irradiation than that observed under sun-like illumination, being comparatively similar to the results shown in Figures 4A and 4B, as is expected, since the catalyst used, BW-Fe(5)-2, is a physical mixture of 95% Bi_2WO_6. Thus, we can conclude that the mechanical mixture of Bi_2WO_6 and α-Fe_2O_3, does not affect the intrinsic photocatalytic behavior observed for single catalysts under the same experimental conditions.

Figures 7C an 7D shows the variation of the MO (Figure 7C) and Phenol (Figure 7D) conversion with time when BW-Fe(5)-2 is usedas aphotocatalystin the co-presence of H_2O_2, under UV or sun-like illumination. A different trend is observed for both substrates. Thus, for MO the simultaneous presence of the mixed catalysts BW-Fe(5)-2 and H_2O_2has a marked influence on the photoassisted discoloration process.This effect is more marked under conditions of UV-illumination for which almost 100%discolorationis achievedin30 min, while high conversion values are obtained (ca. 85% at 60 min) under sun-like irradiation.These conversion values turn out to be higher than those obtained for the same substrate (MO) in homogeneous phase with

light-H_2O_2 (Figure 4A), in the photocatalytic processes using single photocatalysts (Figures5A and 6A) and when the single photocatalysts are used with H_2O_2 (Figures 5C and 6C).These results indicate a synergistic effect in the mixture of the photocatalystsBW-Fe(5)-2 when co-existing with H_2O_2under illumination, at least for the substrate used (MO), since this synergistic effect is not observed for Phenol (Figure 7D).The most striking result is that the synergistic effect occurs even in the visible for MO.

Using this system BW-Fe(5)-2 + H_2O_2, apart from the relatively high values obtained for photo-bleaching of MO, under both UV and under sun-like illumination, relatively high values of mineralization degrees of MO are also obtained(see Table 1).

This fact could be explained by assuming a contribution of photosensitization of a dye moleculesuchas MO, asit has alsobeen observed when using Rhodamine B [31].

As mentioned in the introduction, due to high recombination rate of charge carriers in the single oxides, α-Fe_2O_3 and Bi_2WO_6, have developed strategies that lead to the separation of charge carriers, such as the development of heterostructural constructing of both catalysts [28–30]. In these systems, it has been achieved an improvement in the photocatalytic activity compared with that obtained with the singles catalysts. The α-Fe_2O_3 acts as a hole-accepting semiconductor and photogenerated electrons are injected with high efficiency from the conduction band of α-Fe_2O_3 to the conduction band of Bi_2WO_6. In our work we used a α-Fe_2O_3 / Bi_2WO_6 composite by a mechanical mixing procedure and in order to achieve high performance, the extra H_2O_2 was required. However, the goal is the same in both cases, that is, achieve efficient

separation of the charge carriers. In our case, H_2O_2 acts as an electron acceptor, thus generating •OH radicals while the H_2O can act as holes acceptor, generating more •OH radicals. The advantage, of our method, can be found in the amount of hydroxyl radicals generated in the process, thereby increasing photo-assisted degradation of the substrates. Regardless of this, in our work we have assessed the photocatalytic activity with two different substrates, the MO and Phenol and not with the Rhodamine B, since we have evidence that the evaluation of photocatalytic activity with Rhodamine B generates results that are more spectacular, than when a transparent substrate, such as Phenol is used.

There are other works, that achieve improved photo-Fenton mechanism by incorporating the α-Fe_2O_3 to a graphene oxide (GO) [38] or to Kaolin [39]. In both cases, however, the improvement obtained could be attributed to the synergetic effects of the adsorptive power of GO or Kaolin and the hydroxyl radicals produced by heterogeneous photo-Fenton reactions. In any case, in these works, the evaluation of the activity is done also by using RhB.

Among the mixed catalyst BW-Fe(5)-2,in the presence of H_2O_2, higher conversion values for MOwere displayed, both under UV and sun-like illumination. XPS analyses have been conducted on the prepared mixed oxides system BW-Fe(5)-2, just before and after the photo-assisted Methyl Orange degradation under visible illumination in the presence of hydrogen peroxide, by recovering the catalyst powder from the reaction system, after a prolonged time of illumination (Experiment reported in Figure 7C).

Figure 8 shows the results of XPS analysis of the original sampleofα-Fe_2O_3/Bi_2WO_6, in which only O(1s), W(4f), Bi(4f) and Fe(2p) peaks were detected but no peaks for residual sodium weredetected. The overview

spectrums of the mixed system demonstrate that Bi, W, O and Fe exist, further confirming that the sample was composed of Bi_2WO_6 and Fe_2O_3. As shown in Figure 8A, the characteristic peak of O 1s around 530.1 eV could come from the overlapping contributions of several components, being the identification of the submerged peaks performed by Gaussian deconvolution and curve fitting: these peaks were located at 529.32 eV, 529.65 eV, 530.32 eV, 530.98 eV and 531.26 eV which corresponds to Fe-O, Bi-O, W-O lattice oxygen, chemisorbed water and •OHhydroxyl groups respectively [40,41].

The peaks located at 36.02 eV and 33.91 eV with a spin-orbital separation of 2.11 eV, as shown in Figure 8B, could be assigned to the +6 oxidation state of tungsten for the W $4f_{5/2}$ and $W_{7/2}$respectively [40]. The XPS spectrum of the Bi 4f region displayed in Figure 8C consisting oftwo characteristic peaks with binding energies of 159.04 eV and 164.31 eV correspond to the signals from doublets of Bi $4f_{7/2}$ and Bi $4f_{5/2}$ in the trivalent oxidation state, respectively for pure Bi_2WO_6.

Figure 8D provides XPS peaks of Fe element, exhibiting two individual peaksinthe Fe 2p regionlocated at 710.42 eV and 723.75 eV, which can be assigned to Fe $2p_{3/2}$ and Fe $2p_{1/2}$ peaks in α-Fe_2O_3 phase, respectively [28] confirming the existence of Fe_2O_3 phase on the mixed system which was not detected by XRD technique. Besides two satellite peaks of Fe 2p located at 718.8 eV and 732.9 eV are clearly distinguishable. The satellite peaks were the result of the charge transfer screening attributed to the presence of Fe in 3+ oxidation state [42,43].

However, the splitted peaks of Bi $4f_{7/2}$ and $4f_{5/2}$attributed to Fe^{3+}–O–Bi^{3+} linkage at lower energy values of 157.5 eV and 162.8 eV, respectively[44],donot

appear, indicating that no interaction between α-Fe_2O_3 and Bi_2WO_6existsin the mixed system, as expected by the preparation procedure.

The used α-Fe_2O_3/Bi_2WO_6 sample after photo-assisted discoloration process of Methyl Orange under visible illumination by using H_2O_2, was recovered and, once dried, was subjected to a XPS analysiswith theresultsbeingreported in Figure 9. It is interesting to note that, in the region of the O(1s)peak, two distinct peaks appear centered around 526.8 eV and 530.0 eV respectively. By a deconvolution analysis and fitting, several submerged peaks canbedistinguished. A clear peak centered at 526.58 eV can be attributed to a peroxide species stabilized in the system whichcannot be associated to Na_2O or Na_2O_2[45]since sodium was not detected by XPS. No changes were observed in the oxidation states of W and Bi respectively. However, for this sample, Fe 2p photoelectron peaks appeared around 710.6 eV and 724.0 eV with satellite peaks. The peaks of Fe $2p_{1/2}$ and Fe $2p_{3/2}$ levels at 724.0 eV and 710.6 eV, respectively, separated 13.4 eV, verified the presence of Fe in 3+ oxidation state on the recovered α-Fe_2O_3/Bi_2WO_6 catalysts. However, as shown in Figure 9D, a shoulder around 706.0 eV, not present on the original spectra (Figure 8D) is observed. This could be ascribed to the transformation of Fe(3+) to Fe(2+) after heterogeneous photo-Fenton reaction [46]. This finding, together with the presence of O(1s) peak associated to peroxide species, leadus to postulate the presence of iron(II) peroxide,$Fe(O_2)$,stabilized in the mixed system.

The interaction of H_2O_2 with iron oxide hasnotbeen extensivelystudied, and there are studies that suggest the formation of $Fe(O_2)$ by computer calculations[47,48]; a recent study [49]concluded that the dark Fenton process involving Fe(II) + H_2O_2 consists of two regimes, a fast ferrous one that is

triggered by the reaction of Fe^{2+} + H_2O_2 and a slow ferric one that is dominated by the reduction of Fe(III).However, stabilization of peroxide species as η^2Fe(II) -O_2^{2-} seems unlikely, due to the instability of the peroxide species.

Other proposals could be made, based on results published in the literature [50].Pignatello et al. [51], evidenced the formation of an additional oxidant in the photoassisted Fenton reaction. The results suggest the participation of a high-valentoxoiron complex (ferryl) in addition to •OHin organic compound oxidations.They evidenced that hydrogen peroxide forms a complex with iron, $(Fe^{3+}\text{-}OOH)^{2+}$[K= 1.15 x$10^{-2}$], that absorbs in the visible region and could be the precursor of the proposed ferryl complex[51].

If the formation of $(Fe^{3+}\text{-}OOH)^{2+}$species is assumedthen an increasedphoto-conversion process is likely to occur, in both the UV and visible, as seen in the results presented in Figures 7C and 7D.

3.2.5 Mixtures of Methyl Orange and Phenol

Finally, we have studied the simultaneous degradation of MO and Phenol both ina mixed solution, using the mixed oxide photocatalyst BW-Fe(5)-2, in the presence of H_2O_2undersun-like illumination conditions. Figure 10 reports the variation in the concentration of MO and Phenol in the mixture MO/Phenol with time under sun-like illumination, using the BW-Fe(5)-2 catalyst in the presence of H_2O_2. As noted in Fig.10, it is possible to observe that in mixed solutions of both substrates, there is an increase in Phenol degradation influenced by the simultaneous presence of MO, while the profile of the conversion plot of MO is practically the same as that obtained for the single substrate under the same

experimental conditions (Fig.7C). These results indicate that regardless of the synergistic effect observed in the physical mixture of the two materials studied, BW-Fe(5)-2 in the co-presence of H_2O_2, a marked influence of the simultaneous presence of MO over the Phenol degradation, is also observed.

It is observed that this mixed system, BW-Fe(5)-2, is capable of completely makingMOdisappearin the mixture, after 120 min under sun-like illumination, leading toa residual amount of TOC at the final period, indicating a percentage of 50% of mineralization. From one point of view, having a photosensitizing molecule, suchas MO, has proved to have some effect in the photodegradation of a non-photosensitizing one, like Phenol, since by using these conditions, for single phenol a conversion value of ca. 30% was observed whereas a value of ca. 60% is reached in the co-presence of MO.

Conclusions

Mixed oxides, α-Fe_2O_3/Bi_2WO_6, were prepared using a mechanical mixing procedure by addingthe corresponding amount of a prepared α-$Fe_2O_3$to the Bi_2WO_6previously obtained by hydrothermal method, the former obtainedby thermal decomposition of $Fe(NO_3).9H_2O$.

Despite exhibiting potential optical absorption capacity in the UV-vis region, however, the twosingle catalysts showed poor photocatalytic activity, both in the UV and in the visible, possibly due to high recombination rate of carrier's photo-generated charges. Theprepared oxide α-Fe_2O_3 shows a remarkable dark adsorption capability to MO, however under illumination conditions it displayed a photodesorption process which is accompanied by a simultaneous photo-

catalytic action thatdegrades MO. This α-Fe_2O_3 showed negligible dark adsorption and poor photocatalytic activityfor phenol. However, co-existing with H_2O_2 this oxide is capable of acting as a Fenton-like reagent, expediting the production of substantial amount of hydroxyl radicals. This Fenton-like behavior is not observed when bare Bi_2WO_6 is used.

Beyond a mechanistic approach, it is evident that the mixed oxides BW-Fe (5)-2 co-existing with H_2O_2, enhanced the photocatalytic capability to transform MO, both under UV and sun-like illumination.The generation of •OHdue to the addition of H_2O_2 is crucial not only for MO discoloration but for Phenol transformation.

Mixed oxides BW-Fe(5)-2, co-existing with H_2O_2, has been used in tests involving MO/phenol mixtures, to observe MO photosensitization influence under sun-like irradiation.Eventhough this material, in presence of H_2O_2, was very efficient in MO photo-discoloration, under UV and sun-like, better conversions values are obtained for Phenol whena dye such as MOis co-present.

Although the results by XPS show the formation of peroxidic species, they will be postulated as suggested by Pignatello et al[51]. Clearly, our results indicate the presence of an additional oxidant other than •OH and it could be more evidence to support the assumptions by Pignatello et al.[51].

Acknowledgement

This work was supported by research fund from Project Ref. CTQ2015-64664-C2-2-P(MINECO/FEDER UE) .XPS and others researchservices of CITIUS University of Seville are also acknowledged.

We thank the University of Tolima for economic support in the studies commission of César Augusto Jaramillo Páez.

References

[1] O. Legrini, E. Oliveros, A.M. Braun, Photochemical processes for water treatment, Chem. Rev. 93 (1993) 671–698.

[2] J.H. Sun, S.P. Sun, M.H. Fan, H.Q. Guo, Y.F. Lee, R.X. Sun, Oxidative decomposition of p-nitroaniline in water by solar photo-Fenton advanced oxidation process, J. Hazard. Mater. 153 (2008) 187–193.

[3] J.H. Sun, B. Zhang, R.X. Sun, Y.F. Li, J.F. Wu, Treatment of cornstalk fibrous pulp wastewater using Anaerobic Baffled Reactor (ABR): effect of shock loading rates, Int. J. Environ. Pollut. 38 (2009) 81–87.

[4] S.P. Sun, C.J. Li, J.H. Sun, S.H. Shi, M.H. Fan, Q. Zhou, Decolorization of an azo dye Orange G in aqueous solution by Fenton oxidation process: Effect of system parameters and kinetic study, J. Hazard. Mater. 161 (2009) 1052–1057.

[5] V.K. Gupta, I. Ali, T. a. Saleh, A. Nayak, S. Agarwal, Chemical treatment technologies for waste-water recycling—an overview, RSC Adv. 2 (2012) 6380–6388.

[6] X. Zhou, Y. Li, Y. Zhao, Removal characteristics of organics and nitrogen in a novel four-stage biofilm integrated system for enhanced treatment of coking wastewater under different HRTs, RSC Adv. 4 (2014) 15620–15629.

[7] K. Oudjehani, P. Boule, Photoreactivity of 4-chlorophenol in aqueous solution, J. Photochem. Photobiol. A Chem. 68 (1992) 363–373.

[8] E. Lipczynska-Kochany, J.R. Bolton, Flash photolysis/HPLC method for studying the sequence of photochemical reactions: applications to 4-chlorophenol in aerated aqueous solution, J. Photochem. Photobiol. A Chem. 58 (1991) 315–322.

[9] E. Lipczynska-Kochany, J.R. Bolton, Flash photolysis/HPLC applications. 2. Direct photolysis vs. hydrogen peroxide mediated photodegradation of 4-chlorophenol as studied by a flash photolysis/HPLC technique, Environ. Sci. Technol. 26 (1992) 259–262.

[10] D. Ravelli, D. Dondi, M. Fagnoni, A. Albini, Photocatalysis. A multi-faceted concept for green chemistry., Chem. Soc. Rev. 38 (2009) 1999–2011.

[11] Y. Zhiyong, D. Laub, M. Bensimon, J. Kiwi, Flexible polymer TiO_2 modified film photocatalysts active in the photodegradation of azo-dyes in solution, Inorganica Chim. Acta. 361 (2008) 589–594.

[12] Y. Chen, K. Wang, L. Lou, Photodegradation of dye pollutants on silica gel supported TiO_2 particles under visible light irradiation, J. Photochem. Photobiol. A Chem. 163 (2004) 281–287.

[13] G.A. Rodrigues de Oliveira, J. de Lapuente, E. Teixidó, C. Porredón, M. Borràs, D.P. de Oliveira, Textile dyes induce toxicity on zebrafish early life stages, Environ. Toxicol. Chem. 35 (2015) 429–434.

[14] I. Arslan, A. Balcioglu, Degradation of commercial reactive dyestuffs by heterogenous and homogenous advanced oxidation processes: a comparative study, Dye. Pigment. 43 (1999) 95–108.

[15] G. Ruppert, R. Bauer, G. Heisler, UV-O_3, UV-H_2O_2, UV-TiO_2 and the photo-Fenton reaction - comparison of advanced oxidation processes for wastewater treatment, Chemosphere. 28 (1994) 1447–1454.

[16] K. Wu, Y. Xie, J. Zhao, H. Hidaka, Photo-Fenton degradation of a dye

under visible light irradiation, J. Mol. Catal. A Chem. 144 (1999) 77–84.
[17] M. Neamtu, A. Yediler, I. Siminiceanu, M. Macoveanu, A. Kettrup, Decolorization of disperse red 354 azo dye in water by several oxidation processes - a comparative study, Dye. Pigment. 60 (2004) 61–68.
[18] D. Sannino, V. Vaiano, L.A. Isupova, P. Ciambelli, Heterogeneous Photo-Fenton Oxidation of Organic Pollutants on Structured Catalysts, J. Adv. Oxid. Technol. 15 (2012) 294–300.
[19] S.P. Hu, C.Y. Xu, L. Zhen, Solvothermal synthesis of Bi_2WO_6 hollow structures with excellent visible-light photocatalytic properties, Mater. Lett. 95 (2013) 117–120.
[20] Z. Zhang, M.F. Hossain, T. Takahashi, Fabrication of shape-controlled α-Fe_2O_3 nanostructures by sonoelectrochemical anodization for visible light photocatalytic application, Mater. Lett. 64 (2010) 435–438.
[21] G. V. Buxton, C.L. Greenstock, W.P. Helman, A.B. Ross, Critical Review of rate constants for reactions of hydrated electrons, hydrogen atoms and hydroxyl radicals (OH/O-) in Aqueous Solution, J. Phys. Chem. Ref. Data. 17 (1988) 513–886.
[22] M.D. La Grega, P.L. Buckingham, J.C. Evans, Hazardous Waste Management, Mc Graw Hill, New York, 1994.
[23] S. Esplugas, P.L. Yue, M.I. Pervez, Degradation of 4-chlorophenol by photolytic oxidation, Water Res. 28 (1994) 1323–1328.
[24] U. Bali, E.Ç. Çatalkaya, F. Şengül, Photochemical Degradation and Mineralization of Phenol: A Comparative Study, J. Environ. Sci. Heal. Part A. 38 (2003) 2259–2275.
[25] S. Dong, J. Feng, M. Fan, Y. Pi, L. Hu, X. Han, et al., Recent developments in heterogeneous photocatalytic water treatment using visible light-responsive photocatalysts: a review, RSC Adv. 5 (2015) 14610–14630.
[26] K. Sahel, L. Elsellami, I. Mirali, F. Dappozze, M. Bouhent, C. Guillard, Hydrogen peroxide and photocatalysis, Appl. Catal. B Environ. 188 (2016) 106–112.
[27] J. Sheng, X. Li, Y. Xu, Generation of H_2O_2 and OH Radicals on Bi_2WO_6 for Phenol Degradation under Visible Light, ACS Catal. 4 (2014) 732–737.
[28] Y. Guo, G. Zhang, J. Liu, Y. Zhang, Hierarchically structured α-Fe_2O_3/Bi_2WO_6 composite for photocatalytic degradation of organic contaminants under visible light irradiation, RSC Adv. 3 (2013) 2963–2970.
[29] Q.S. Wu, Y. Feng, G.Y. Zhang, Y.Q. Sun, Y.Y. Xu, D.Z. Gao, α-Fe_2O_3 modified Bi_2WO_6 flower-like mesostructures with enhanced photocatalytic performance, Mater. Res. Bull. 49 (2014) 440–447.
[30] X.N. Liu, Q.F. Lu, C.F. Zhu, S.W. Liu, Enhanced photocatalytic activity of α-Fe_2O_3/Bi_2WO_6 heterostructured nanofibers prepared by electrospinning technique, RSC Adv. 5 (2015) 4077–4082.
[31] S. Murcia-López, M.C. Hidalgo, J.A. Navío, Degradation of Rhodamine B/Phenol Mixtures in Water by Sun-Like Excitation of a Bi_2WO_6-TiO_2 Photocatalyst, Photochem. Photobiol. 89 (2013) 832–840.
[32] D.M. Sherman, T.D. Waite, Electronic spectra of Fe^{3+} oxides and oxide hydroxides in the near IR to near UV., Am. Mineral. 70 (1985) 1262–1269.
[33] G. Colón, S. Murcia López, M.C. Hidalgo, J.A. Navío, Sunlight highly photoactive Bi_2WO_6-TiO_2 heterostructures for rhodamine B degradation.,

Chem. Commun. 46 (2010) 4809–4811.
[34] S. Murcia López, M.C. Hidalgo, J.A. Navío, G. Colón, Novel Bi_2WO_6-TiO_2 heterostructures for Rhodamine B degradation under sunlike irradiation, J. Hazard. Mater. 185 (2011) 1425–1434.
[35] C. Kormann, D.W. Bahnemann, M.R. Hoffmann, Environmental Photochemistry - Is Iron-Oxide (Hematite) an Active Photocatalyst? A Comparative Study α-Fe_2O_3, ZnO, TiO_2, J. Photochem. Photobiol. A-Chemistry. 48 (1989) 161–169.
[36] C. Siffert, B. Sulzberger, Light-induced dissolution of hematite in the presence of oxalate. A case study, Langmuir. 7 (1991) 1627–1634.
[37] M.I. Litter, J.A. Navío, Photocatalytic properties of iron-doped titania semiconductors, J. Photochem. Photobiol. A Chem. 98 (1996) 171–181.
[38] S. Guo, G. Zhang, Y. Guo, J.C. Yu, Graphene oxide-Fe_2O_3 hybrid material as highly efficient heterogeneous catalyst for degradation of organic contaminants, Carbon N. Y. 60 (2013) 437–444.
[39] S. Guo, G. Zhang, J. Wang, Photo-Fenton degradation of rhodamine B using Fe_2O_3-Kaolin as heterogeneous catalyst: Characterization, process optimization and mechanism, J. Colloid Interface Sci. 433 (2014) 1–8.
[40] D. Wang, Y. Zhen, G. Xue, F. Fu, X. Liu, D. Li, Synthesis of mesoporous Bi2WO6 architectures and their gas sensitivity to ethanol, J. Mater. Chem. C. 1 (2013) 4153–4162.
[41] S. Guo, X. Li, H. Wang, F. Dong, Z. Wu, Fe-ions modified mesoporous Bi_2WO_6 nanosheets with high visible light photocatalytic activity., J. Colloid Interface Sci. 369 (2012) 373–380.
[42] Y. Jia, T. Luo, X.-Y. Yu, Z. Jin, B. Sun, J.-H. Liu, et al., Facile one-pot synthesis of lepidocrocite (γ-FeOOH) nanoflakes for water treatment, New J. Chem. 37 (2013) 2551–2556.
[43] L. Li, Y. Chu, Y. Liu, L. Dong, Template-Free Synthesis and Photocatalytic Properties of Novel Fe_2O_3 Hollow Spheres, J. Phys. Chem. C. 111 (2007) 2123–2127.
[44] M. Aslam, M.T. Soomro, I.M.I. Ismail, H.A. Qari, M.A. Gondal, A. Hameed, The facile synthesis, characterization and evaluation of photocatalytic activity of bimetallic $FeBiO_3$ in natural sunlight exposure, RSC Adv. 5 (2015) 102663–102673.
[45] F. Klein, R. Pinedo, P. Hering, A. Polity, J. Janek, P. Adelhelm, Reaction Mechanism and Surface Film Formation of Conversion Materials for Lithium- and Sodium-Ion Batteries: A XPS Case Study on Sputtered Copper Oxide (CuO) Thin Film Model Electrodes, J. Phys. Chem. C. 120 (2016) 1400–1414.
[46] J. Deng, J. Jiang, Y. Zhang, X. Lin, C. Du, Y. Xiong, $FeVO_4$ as a highly active heterogeneous Fenton-like catalyst towards the degradation of Orange II, Appl. Catal. B Environ. 84 (2008) 468–473.
[47] A.T. García-Sosa, M. Castro, Density Functional Study of FeO_2, FeO_2^+ , and FeO^-_2, Int. J. Quantum Chem. 80 (2000) 307–319.
[48] T. Nakazawa, Y. Kaji, A density functional theory investigation of the reactions of Fe and FeO_2 with O_2, Comput. Mater. Sci. 117 (2016) 455–467.
[49] C. Minero, M. Lucchiari, V. Maurino, D. Vione, A quantitative assessment of the production of ˙OH and additional oxidants in the dark Fenton reaction: Fenton degradation of aromatic amines, RSC Adv. 3 (2013)

26443–26450.
[50] J.J. Pignatello, E. Oliveros, A. MacKay, Advanced Oxidation Processes for Organic Contaminant Destruction Based on the Fenton Reaction and Related Chemistry, Crit. Rev. Environ. Sci. Technol. 36 (2006) 1–84.
[51] J.J. Pignatello, D. Liu, P. Huston, Evidence for an additional oxidant in the photoassisted Fenton reaction, Environ. Sci. Technol. 33 (1999) 1832–1839.

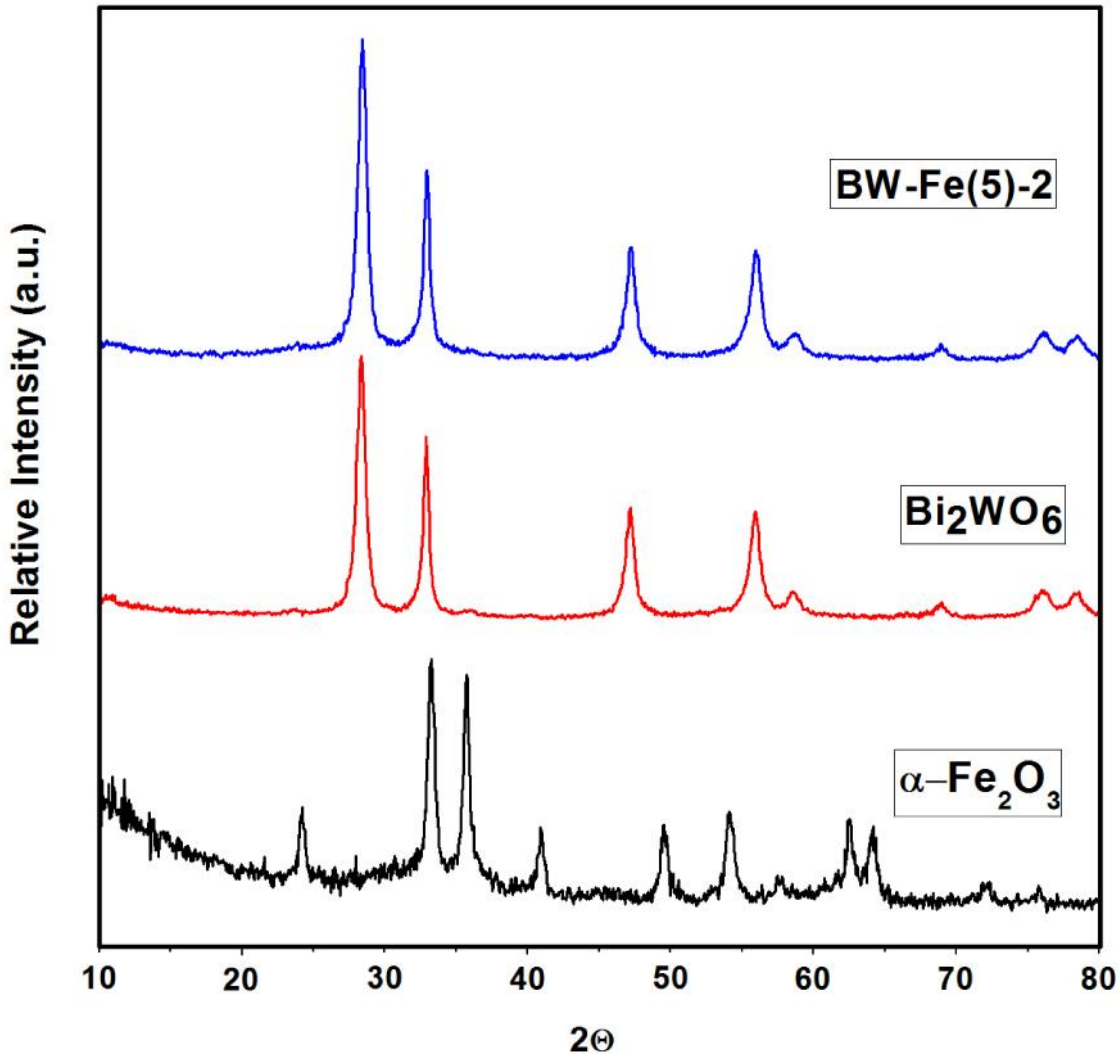

Figure 1. X-ray diffraction patterns (XRD) of pristine α-Fe_2O_3, Bi_2WO_6 and mixed BW-Fe(5)-2 samples

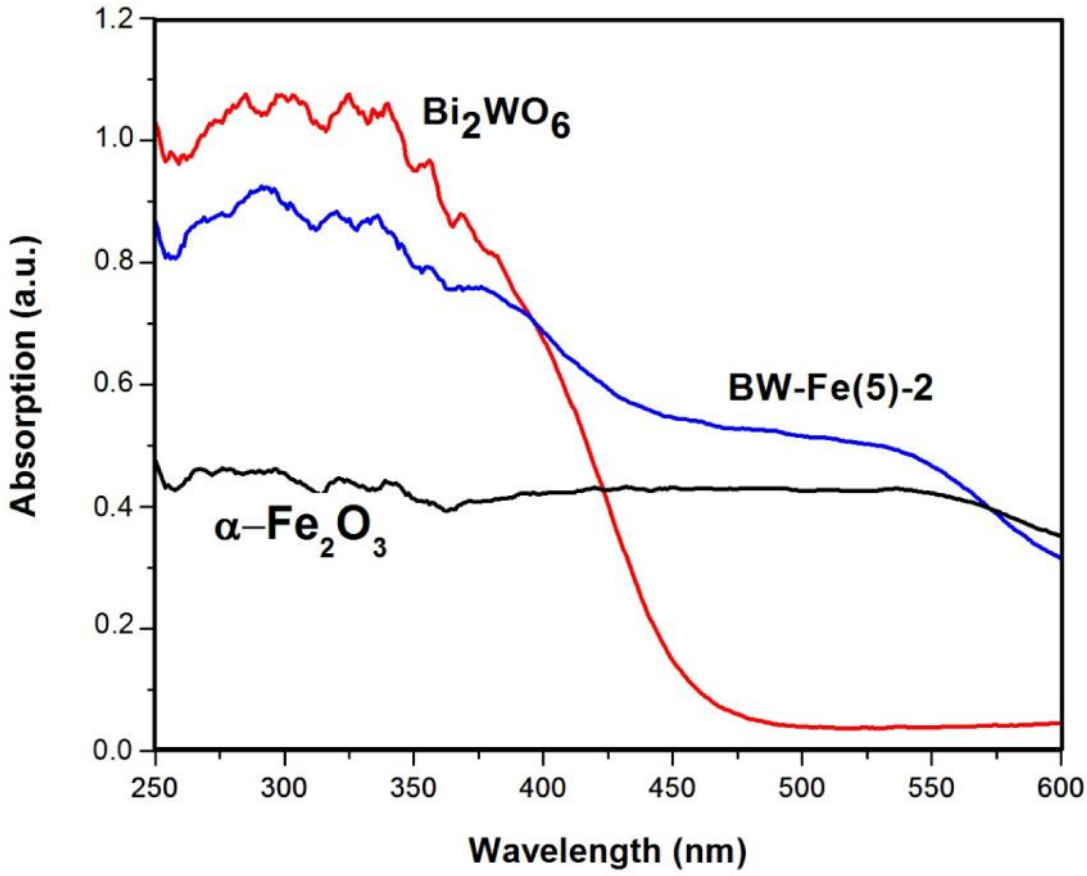

Figure 2. Diffused reflectance spectra (DRS) of pristine α-Fe_2O_3, $Bi_2WO_6$and mixed BW-Fe(5)-2 samples.

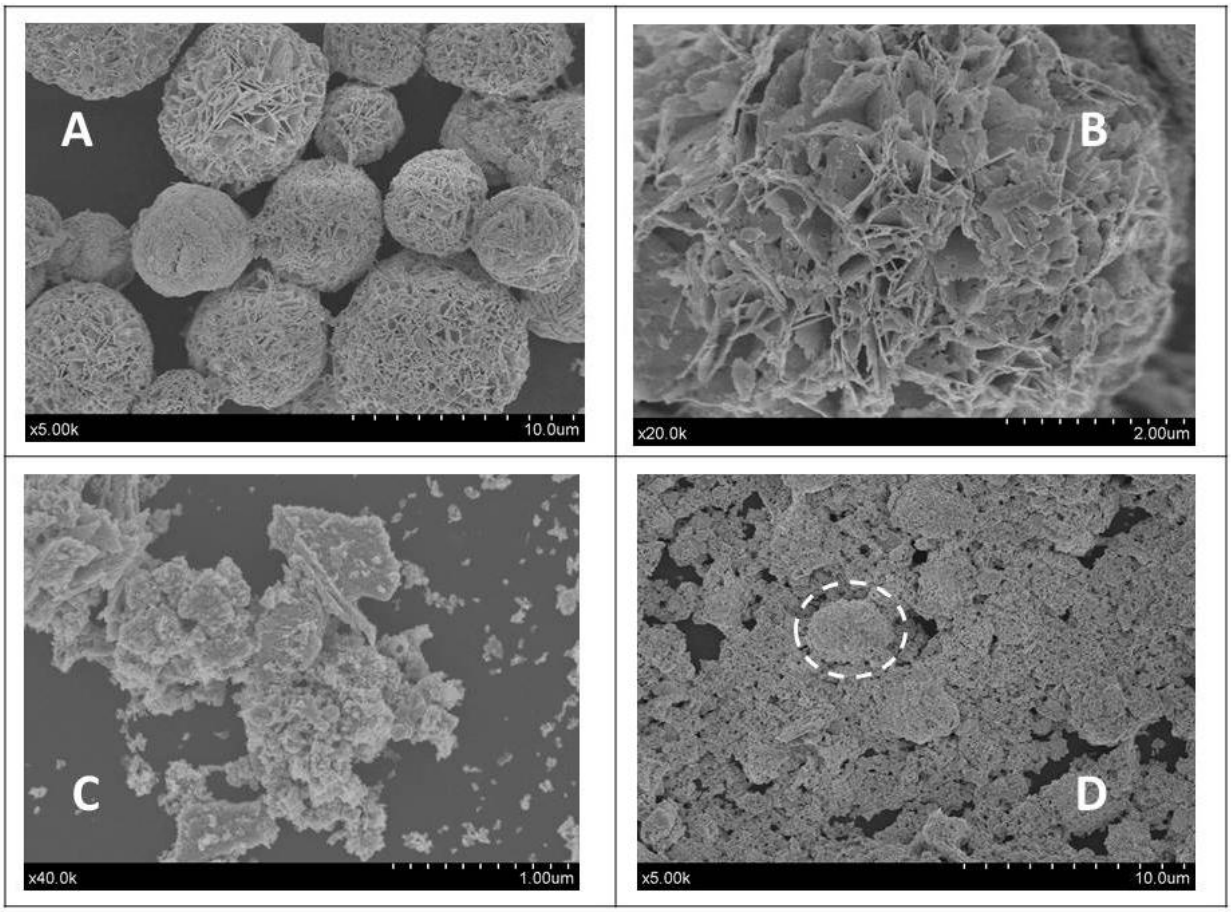

Figure 3.SEM images of pristine Bi_2WO_6 (A and B), pristine α-Fe_2O_3 (C), and mixed BW-Fe(5)-2 samples (D).

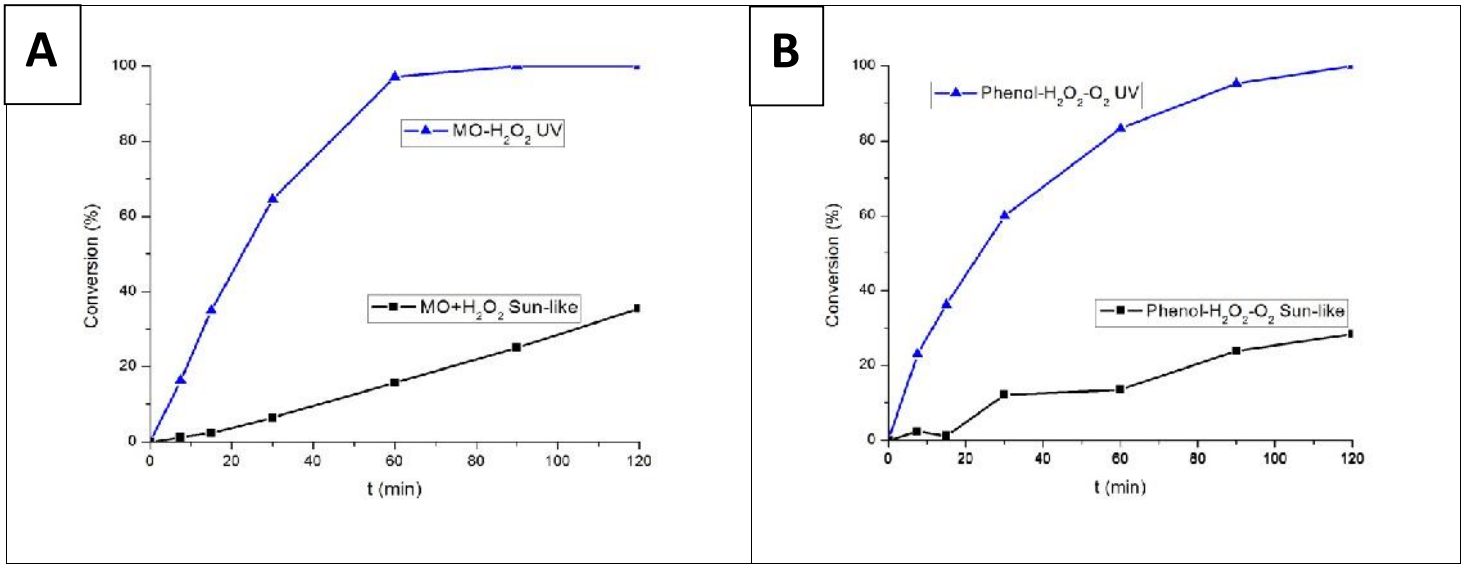

Figure 4. Conversion plots for photochemical discoloration of Methyl Orange (A) and photochemical disappearance of Phenol (B), with only the presence of H_2O_2 under UV or sun-like illumination.

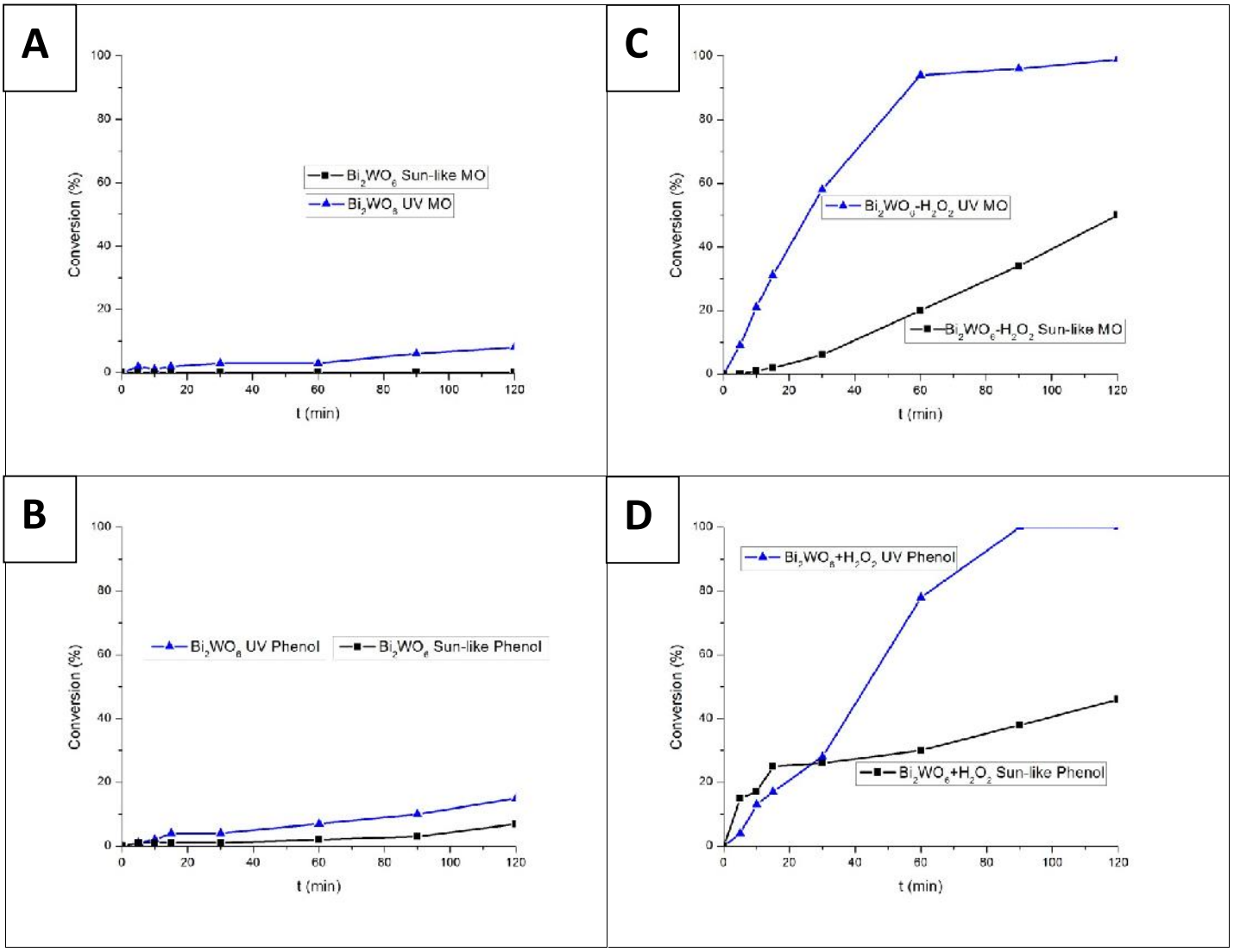

Figure 5. Conversion plots for photochemical discoloration of Methyl Orange and Phenol disappearance, under UV or sun-like illumination: with only the presence of Bi_2WO_6 photocatalyst (A and B) or with the co-presence of both, Bi_2WO_6 and H_2O_2 (C and D).

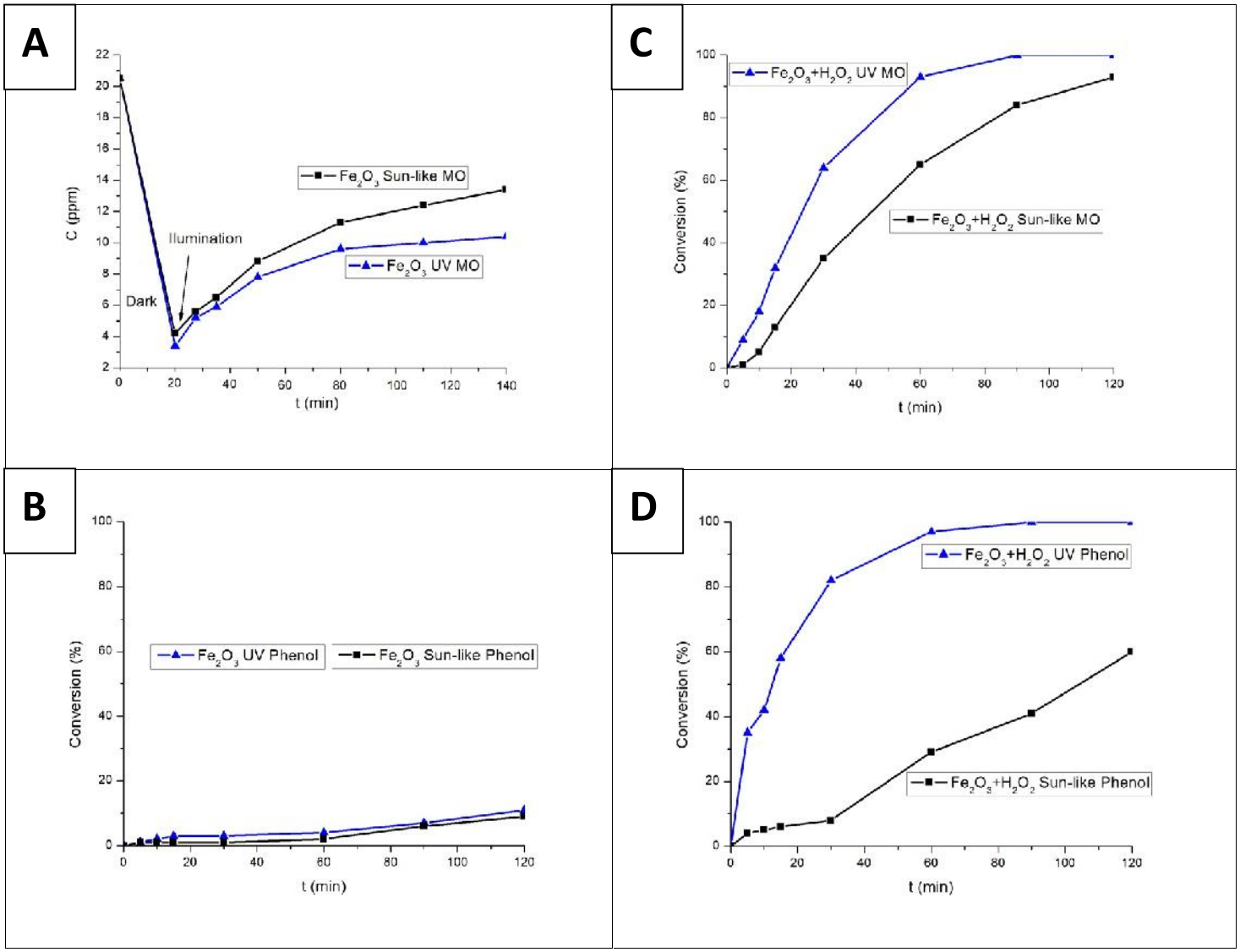

Figure 6. Conversion plots for photochemical discoloration of Methyl Orange and Phenol disappearance, under UV or sun-like illumination: with only the presence of α-Fe_2O_3 photocatalyst (A and B) or with the co-presence of both, α-Fe_2O_3 and H_2O_2 (C and D).

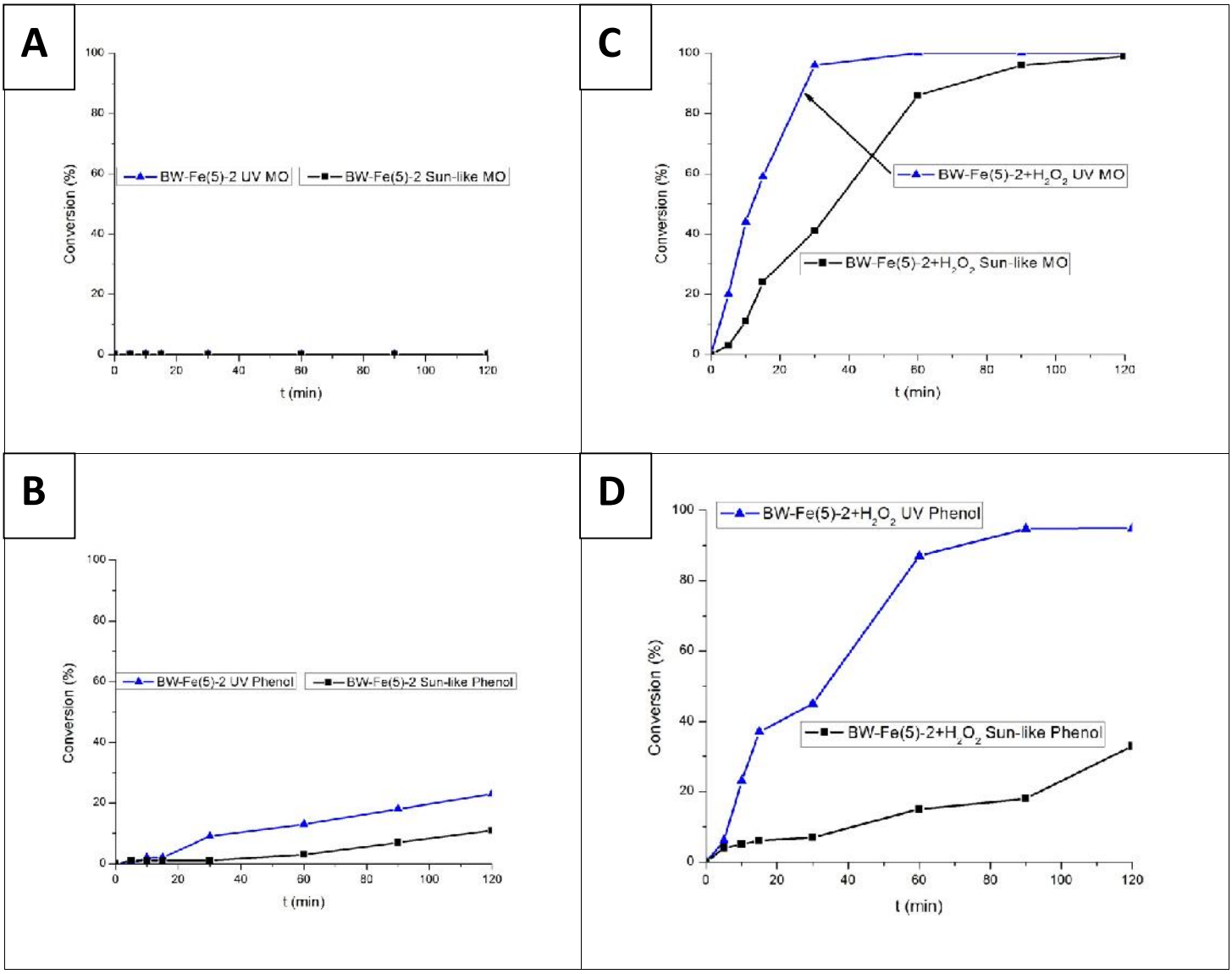

Figure 7. Conversion plots for photochemical discoloration of Methyl Orange and Phenol disappearance, under UV or sun-like illumination: with only the presence of mixed BW-Fe(5)-2 photocatalysts (A and B) or with the co-presence of BW-Fe(5)-2 photocatalysts and H_2O_2 (C and D).

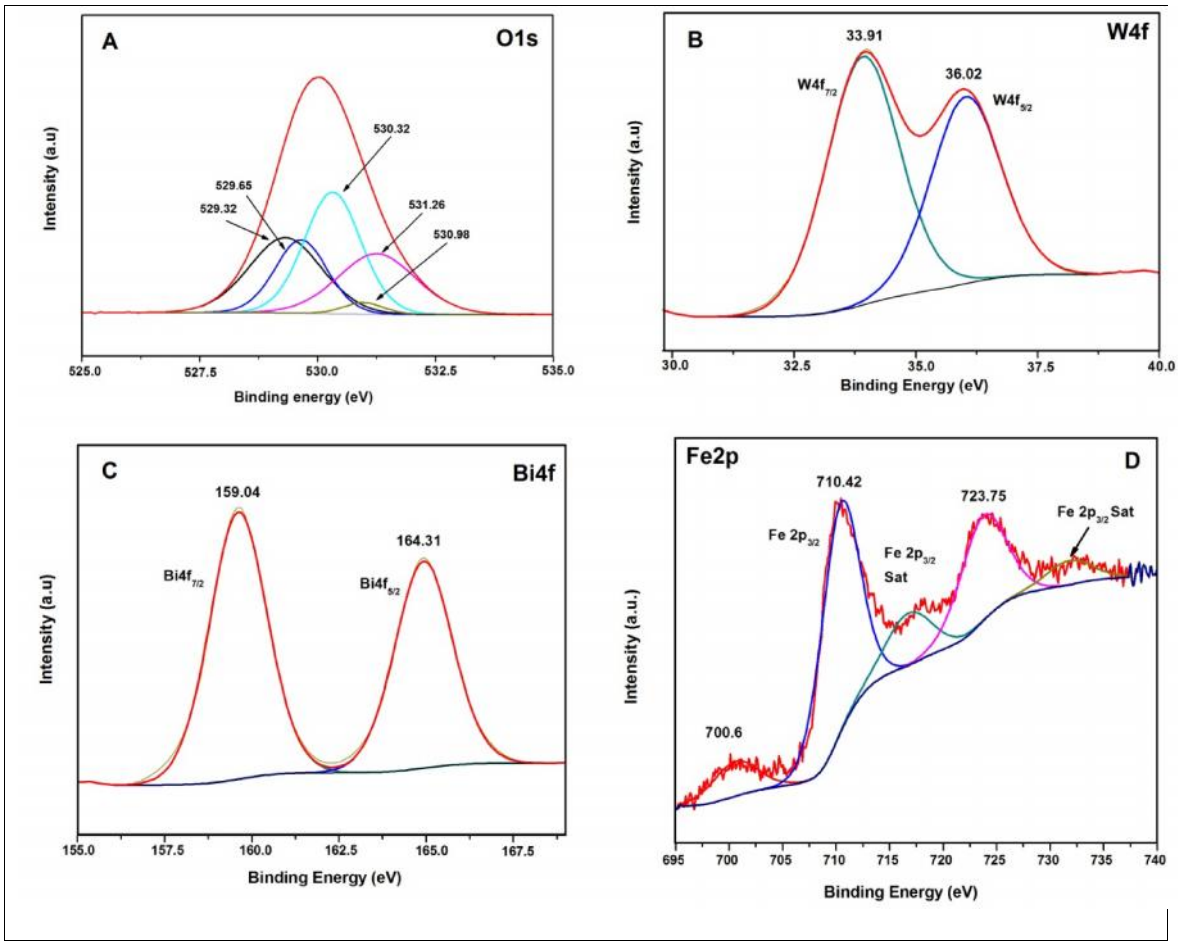

Figure 8. XPS surface spectra of the as-prepared mixed BW-Fe(5)-2 photocatalysts.

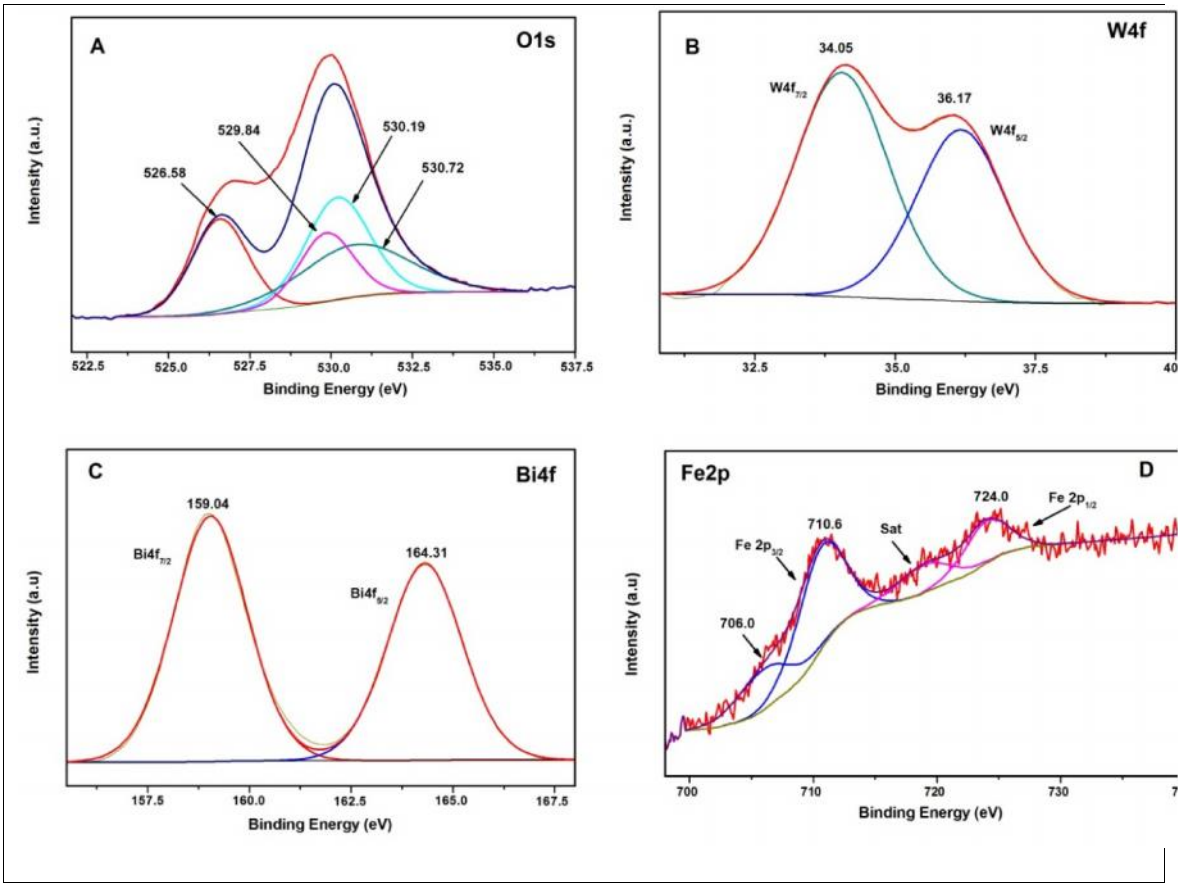

Figure 9. XPS surface spectra of the recoveredBW-Fe(5)-2 sample after being used on the photo-assisted discoloration process of Methyl Orange under visible illumination by using H_2O_2.

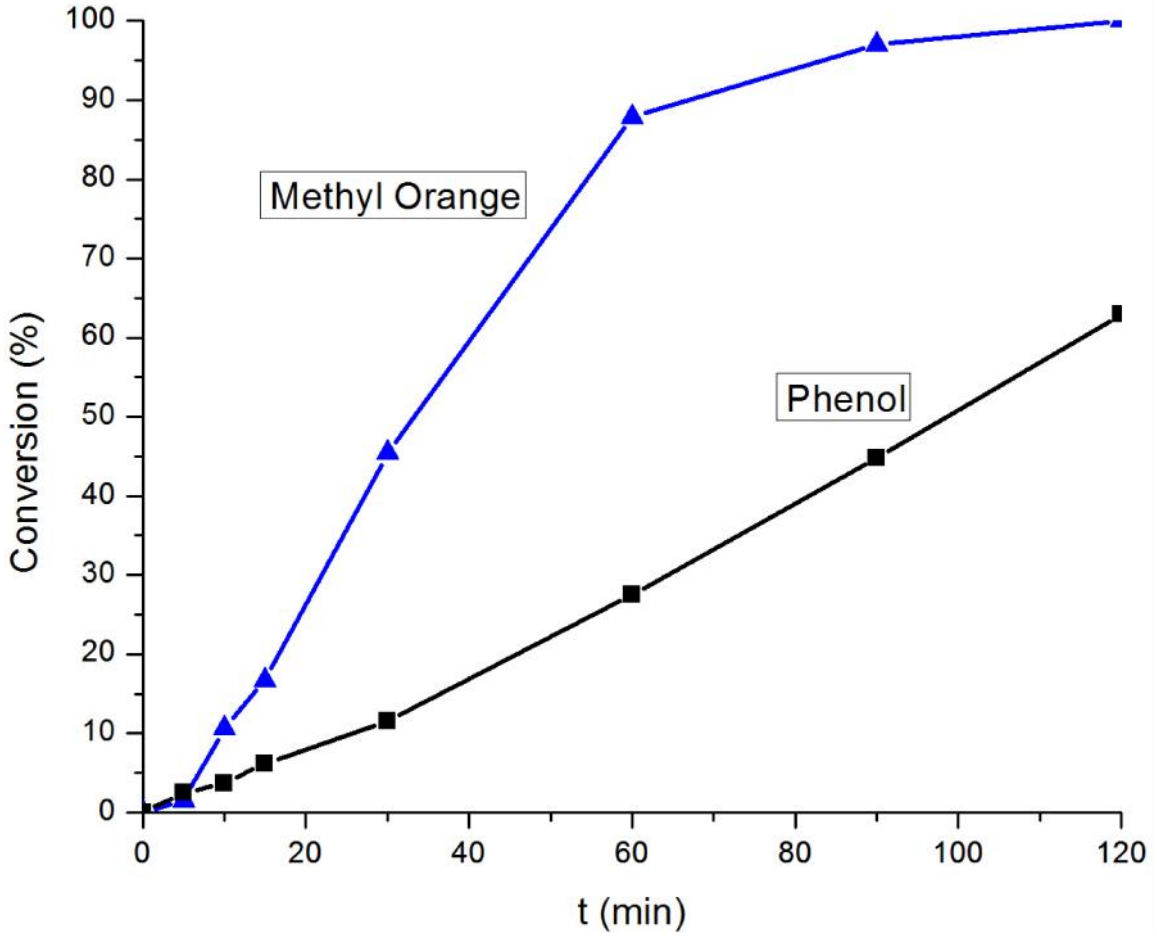

Figure 10. Methyl Orange and Phenol conversion plots in mixed solution with BW-Fe(5)-2 under sun-like illumination, in the presence of H_2O_2

Table 1. Mineralization (%) obtained from the TOC values upon 2 h of irradiation of the studied systems.

SYSTEM	**Mineralization (%)** **[1 − (final TOC/initialTOC)]x100**
MO (20) + H_2O_2-UV	54.0
MO (20) + H_2O_2 Sun-like	39.1
Ph (50) + H_2O_2-UV	49.0
Ph (50) + H_2O_2-Vis	26.5
(MO) Bi_2WO_6-UV	14.6
(MO) Bi_2WO_6 Sun-like	5.5
(Ph) Bi_2WO_6-UV	59.5
(Ph) Bi_2WO_6 Sun-like	37.9
(MO) Bi_2WO_6-H_2O_2 UV	68.1
(MO) Bi_2WO_6-H_2O_2 Sun-like	68.1
(Ph) Bi_2WO_6-H_2O_2 UV	68.3
(Ph) Bi_2WO_6-H_2O_2 Sun-like	55.2
(MO) Fe_2O_3 UV	27.0
(MO) Fe_2O_3 Sun-like	27.4
(Ph) Fe_2O_3 UV	35.1
(Ph) Fe_2O_3 Sun-like	25.5

(MO) Fe_2O_3-H_2O_2 UV	67.8
(MO) Fe_2O_3-H_2O_2Sun-like	46.7
(Ph) Fe_2O_3-H_2O_2 UV	68.1
(Ph) Fe_2O_3-H_2O_2Sun-like	49.3
(MO) Bi_2WO_6-Fe_2O_3 UV	10.0
(MO) Bi_2WO_6-Fe_2O_3 Sun-like	5.0
(Ph) $B_{i2}WO_6$-Fe_2O_3 UV	32.0
(Ph) Bi_2WO_6-Fe_2O_3 Sun-like	21.1
(MO) Bi_2WO_6-Fe_2O_3 + H_2O_2 UV	69.6
(MO) Bi_2WO_6-Fe_2O_3+ H_2O_2Sun-like	46.4
(Ph) Bi_2WO_6-Fe_2O_3+ H_2O_2 UV	70.0
(Ph) Bi_2WO_6-Fe_2O_3 + H_2O_2Sun-like	41.0
(MO +Ph) 10:20 Bi_2WO_6-Fe_2O_3 + H_2O_2 Sun-like	50.7